Molecular Crystals and Liquid Crystals
Publication details, including instructions for authors and subscription information:
http://www.tandfonline.com/loi/gmcl20

Enhanced Efficiency in Dye-Sensitized Solar Cells Based on TiO_2 Nanotube Scattering Layer

Chang Hyo Lee [a] & Hyung Wook Choi [a]

[a] Department of Electrical Engineering, Gachon University, Seongnamdaero 1342, Sujeong-gu, Seongnam, Gyeonggi-do, 461-701, Korea

Version of record first published: 30 Aug 2012.

To cite this article: Chang Hyo Lee & Hyung Wook Choi (2012): Enhanced Efficiency in Dye-Sensitized Solar Cells Based on TiO_2 Nanotube Scattering Layer, Molecular Crystals and Liquid Crystals, 565:1, 124-130

To link to this article: http://dx.doi.org/10.1080/15421406.2012.693305

Mol. Cryst. Liq. Cryst., Vol. 565: pp. 124–130, 2012

ISSN: 1542-1406 print/1563-5287 online
DOI: 10.1080/15421406.2012.693305

Taylor & Francis
Taylor & Francis Group

Enhanced Efficiency in Dye-Sensitized Solar Cells Based on TiO_2 Nanotube Scattering Layer

CHANG HYO LEE AND HYUNG WOOK CHOI*

Department of Electrical Engineering, Gachon University, Seongnamdaero 1342, Sujeong-gu, Seongnam, Gyeonggi-do 461-701, Korea

The essential goal for the production of dye-sensitized solar cells (DSSCs) is to improve the light-scattering ability of these films. Therefore, transparent high surface area TiO_2 layers and an additional scattering layer consisting of TiO_2 nanotubes (TNTs) with relatively larger particles are attractive. The light-scattering abilities of these scattering layers also depend on the relative sizes and the phase of the particles in the layers. TNTs were fabricated by a sol-gel method, and the TiO_2 powders were produced through an alkali hydrothermal transformation. The size and structure of the TNTs were adjusted by the hydrothermal temperatures. It was observed that the TiO_2 films transformed into the rutile phase, which has a more stable structure, as the temperature increases. This study examined the scattering efficiency in terms of the size, crystal phase, and morphology of the scattering particle. With a 6 μm-thin titanium dioxide semiconductor layer as a photoelectrode and an additional light-scattering layer (consisting of TNTs-rutile large-size particle), efficiencies of 4.4% were achieved.

Keywords Dye- sensitized solar cells; hydrothermal method; TiO_2 nanotube; scattering layer

Introduction

Dye-sensitized solar cells (DSSCs) have been studied intensively since their discovery in 1991 for use in a new generation of energy harvesting devices because of their simple structure and process, low-cost fabrication, transparency, color control, and applicability in flexible DSSCs [1–4]. DSSCs consist of a wide band gap mesoporous metal oxide film, such as TiO_2, deposited on a conducting oxide layer as an electron transport layer with an organic dye as a sensitizer, such as ruthenium; an electrolyte as an ionic electron conductor, such as iodolyte; and a high work-function metal as the counter electrode, such as platinum. Nanoporous TiO_2 is commonly used in DSSCs to embed a high density of dye molecules onto the TiO_2 surface to enhance the photo -absorption process [5]. Grätzel et al. introduced mesoporous TiO_2 films as photoanodes to enhance the effective surface area, to absorb more dye molecules, and to achieve more light absorption and greater efficiency [6,7]. The energy conversion efficiency is likely to be dependent on the morphology and structure of the dye-adsorbed TiO_2 film. Whereas, increasing the surface area by simply increasing the film thickness is restricted since the increased surface states induced by the increased surface

*Address correspondence to Prof. Hyung Wook Choi, Department of Electrical Engineering, Gachon University, Seongnamdaero 1342, Sujeong-gu, SeongNam, Gyeonggi-do 461-701, Korea (ROK). Tel.: (+82)31-750-5562; Fax: (+82)31-750-5491. E-mail: chw@ gachon.ac.kr

area act as recombination centers of photo-injected electrons [8–10]. Therefore, extending the retention period of light in DSSCs by creating a light-scattering layer in the working electrode is one of the promising approaches to enhance the performance of DSSCs. For example, Ito et al. proposed a photon-trapping system, which consisted of a transparent layer of nanocrystalline TiO_2 particles and a light-scattering layer of microcrystalline anatase particles [11]. The light-scattering abilities of these scattering layers also depend on the relative sizes of the particles in the layers [12].

In the study, the TNTs were then applied in the scattering layer of a DSSCs, and the effect of particle size of TNTs on the performance of a DSSC was investigated. TiO_2 nanoparticles were fabricated by a sol-gel method, and the TNTs were produced through an alkali hydrothermal transformation. The size and structure of the TNTs were adjusted by the hydrothermal temperatures [13,14]. A comparison of a DSSC with the proposed scattering layer with the conventional DSSCs was also made.

Experimental Procedures

The TiO_2 main-layer was prepared using the sol-gel method. Nano TiO_2 was synthesized using titanium (IV) isopropoxide [TTIP (Aldrich Chemical)], nitric acid, ethyl alcohol, and distilled water. The TTIP was mixed with ethanol, and distilled water was added dropwise under vigorous stirring for 1 h. This solution was peptized using nitric acid and heated under reflux at 80°C for 8 h. After this period, the TiO_2 sol was prepared. The prepared sol was dried to yield a TiO_2 powder. The TiO_2 powder was calcined in air at 450°C for 1 h, using a programmable furnace to obtain the desired stoichiometry and crystallinity of the TiO_2.

The TNTs scattering layer was prepared using a hydrothermal method. TiO_2 powders in the amount of 5 g were prepared by the sol-gel method and mixed with 500 ml of a 10 M NaOH aqueous solution followed by a hydrothermal treatment at 120°C (TNTa), 150°C (TNTb), and 200°C (TNTc) in a Teflon-lined autoclave for 24 h. After the hydrothermal reaction, the treated powders were washed thoroughly with distilled water and 0.1 M HCl, and subsequently, filtered and dried at 80°C for 1 day. To achieve the desired size and crystallinity of the TNT (a, b, c), the powders were calcinated in air at 500°C for 1 h. To examine the effect of the scattering particle size on the light-scattering efficiency, acetic acid (1 ml), distilled water (5 ml), and ethanol (30 ml) were added dropwise to disperse the TiO_2 powders and TNTs under continuous grinding. The TiO_2 dispersions in the mortar were transferred with an excess of ethanol (100 ml) to a tall beaker and stirred with a 4 cm-long magnet tip at 300 rpm. Anhydrous terpineol (20 g) and ethyl celluloses (3 g) in ethanol were added, followed by further stirring. The contents in the dispersion were concentrated by evaporating ethanol with a rotary evaporator. The pastes were finished by grinding in a three-roller mill [15]. Optically transparent conducting glass [FTO (fluorine doped SnO_2, sheet resistance 8 Ω/sq)] was washed in ethanol and (DI) water in an ultrasonic bath for 10 min. The prepared paste was then coated on the FTO conductive glass by screen printing. The thermal treatment at 450°C for 15 min and at 500°C for 15 min was performed to completely remove the incorporated elemental carbon through a chemical reaction with oxygen. Three types of TNTs scattering particles, TNTa, TNTb, and TNTc, with various particle sizes, were used. Screen printable pastes containing the TNTs (a, b, c) were also prepared using the same procedure described above.

The phase of the particles obtained at various hydrothermal temperatures was examined by X-ray diffraction (XRD) using a Rigaku D/MAX-2200 diffractometer with CuKα

radiation. The morphology and thickness of the prepared TNTs layers were investigated by field-emission scanning electron microscopy (FE-SEM, model S-4700, HITACHI). The absorption spectra and transmittance TiO_2 films were measured using a UV-vis spectrometer (UV-vis 8453, Agilent). The conversion efficiency of the fabricated DSSC was measured using an I-V solar simulator (solar simulator, McScience).

Results and Discussion

XRD of the sol-gel TiO_2 powders at 450°C revealed a mixture of anatase and rutile (Fig. 1a). In Fig. 1(b, c, d), the films were calcined in air at 500°C for 1 h, using a programmable furnace to obtain the desired size and crystallinity of the TNTs. TNTa (120°C) is a mixture of anatase and rutile. The XRD pattern of TNTb (150°C) showed a prominent anatase peak at 25.4° (101) and 48° (200). In contrast, the XRD pattern of TNTc (200°C) showed a prominent rutile peak at 27.4° (110) and 54.2° (211). With TNTc, the anatase peaks almost disappeared, whereas the intensities of the rutile peaks increased considerably, indicating that the anatase to rutile transformation was complete. The TiO_2 films transformed into the more stable rutile phase as the temperature ware increased. The crystallized direction intensity changes under different hydrothermal temperatures.

FE-SEM was used to examine the TiO_2 layers prepared at various working pressures as well as the TiO_2 nanoparticle sol-gel and TNTs films prepared at various hydrothermal temperatures. The diameter of the TiO_2 powder prepared by the sol-gel method was 20–25 nm (Fig. 2a). The TiO_2 particles exhibit tubular shapes (Fig. 2b, c, d). The TNTs film prepared at 120°C showed a small diameter (Fig. 2b). Figure 2c shows a FE-SEM image of an anatase TNTs film. The rutile TNTs film at 200°C showed a large diameter (Fig. 2d). SEM showed that the grain size of the rutile phase was larger than that of the anatase phase. The TiO_2 film transformed into the rutile as the hydrothermal temperature was increased.

Figure 3 shows the cross-section of the light-scattering layer by crystalline-TNTs. FE-SEM indicated four parts. The top one is the TNTs scattering layer, 1–2 μm in thickness. Figure 4 shows the transmittance spectra of the films of TiO_2 with and without the scattering

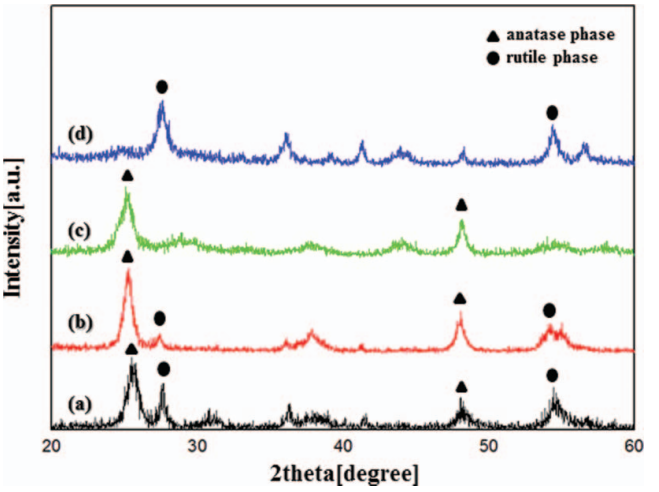

Figure 1. XRD patterns of the TiO_2 nanoparticle by sol-gel method and TiO_2 nanotube films at various hydrothermal temperatures (▲ : anatase phase, ● : rutile phase).

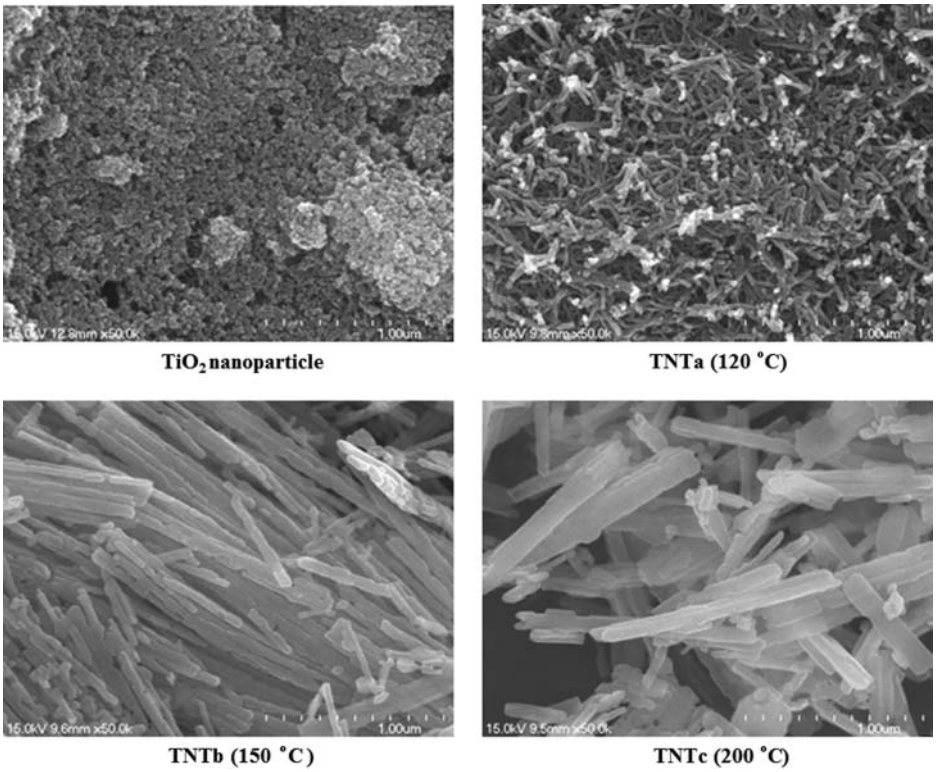

Figure 2. FE-SEM images of the TiO_2 nanoparticle and TiO_2 nanotube films at various hydrothermal temperatures : (a) TiO_2, (b) 120°C, (c) 150°C, and (d) 200°C.

layers. The transmittance of the films decreased as more scattering layers were added. In addition, the total transmittance decreased due to the increase in the particle size of scattering layers.

Figure 5 shows the absorption spectrum of N-719 dye in the 400–800 nm-wavelength range in the flexible TiO_2 electrode film with various size TNTs scattering particles. It can

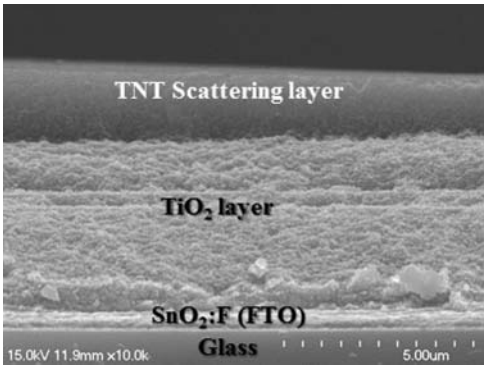

Figure 3. FE-SEM images of the cross-section of the light-scattering layer by crystalline-TNT.

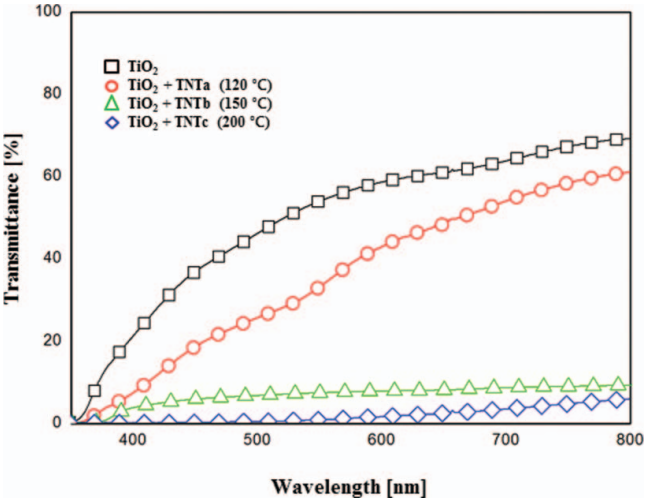

Figure 4. Optical transmittance of the TiO_2 layer with and without the scattering layers.

be seen in Fig. 5 that in the 400–500 nm-wavelength range, the sample basic TiO_2 film and TiO_2/TNT (a, b) showed the higher absorbance, and the sample TNTc showed the lowest absorbance. Due to large particle sizes of the scattering particles, these layers have low surface area, and they render virtually no dye adherence.

Figure 6 shows current-voltage curves of DSSCs obtained under 100 mW/cm^2 illumination with AM 1.5 G of the DSSCs fabricated by different temperatures using the TiO_2 main-layer with the TNTs scattering layer. In addition, Table 1 summarizes the efficiency, fill factor, open-circuit voltage, and integral photocurrent for the corresponding solar cells.

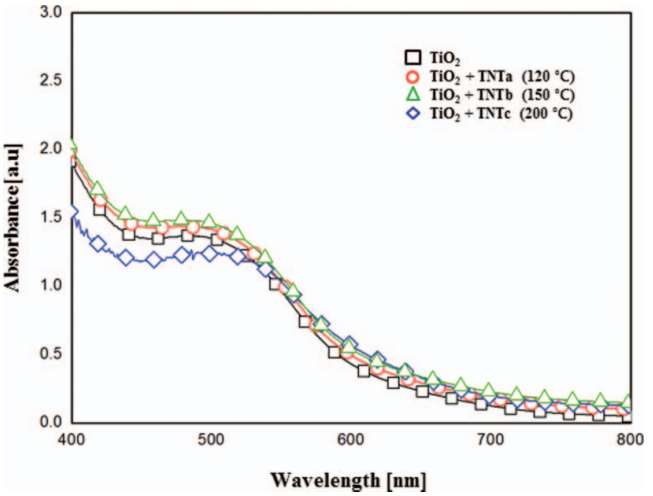

Figure 5. Absorption spectra of dye N719 desorbed from the TiO_2 layer with and without the scattering layers.

Table 1. The photovoltaic parameters of the DSSCs prepared with TiO_2 + TNTs scattering layer with the TiO_2 layer.

	Voc (V)	Jsc (mA/cm^2)	FF (%)	η (%)
TiO_2	0.65	9.35	64.01	3.89
TiO_2+TNTa (120°C)	0.64	9.11	62.71	3.66
TiO_2+TNTb (150°C)	0.65	9.85	65.29	4.18
TiO_2+TNTc (200°C)	0.63	10.71	65.23	4.40

The scattering efficiency of rutile and anatase particles, the large-size rutile particle-based scattering layer exhibited a slightly higher photocurrent density than the anatase-based one, which is associated with the higher refractive index of rutile. Therefore, an increase in current density and cell efficiency of 4.4% were obtain using a 4 μm-thin TiO_2 film with a high surface area together with an efficient light-scattering layer (consisting of TNTc-Rutile). The nanocrystalline TiO_2 film with high surface area is able to utilize more photons because of the high quantity of the adsorbed dye. In contrast, the considerably lower efficiency in the TiO_2 + TNT (a, b) samples was associated with inferior electron transport and recombination properties due to the random array of smaller TNTs, despite the enormous light absorbance [16,17]. As a result, the optimum condition for high conversion efficiency was a TiO_2 film containing TNTc light-scattering particles. Eventually, the scattering effect of the large TNTs enhances the photocurrent density and thereby, the overall conversion efficiency.

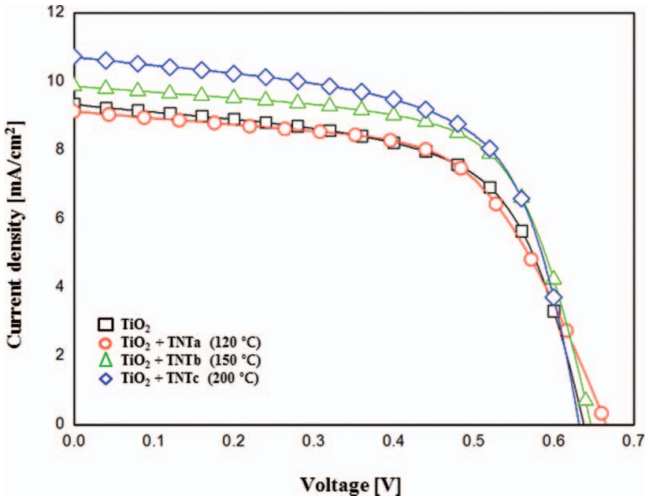

Figure 6. The photocurrent and voltage curves of the DSSCs prepared TiO_2 + TNTs scattering layer with the TiO_2 layer.

Conclusions

The photovoltaic performances of DSSC based on a 4 μm-thick TiO_2 layer with and without light-scattering layers were compared. The potential of the scattering layers of various sizes with respect to efficient light collection in the device were considered. The size and structure of the TiO_2 nanotube were adjusted by the hydrothermal temperatures. Anatase was formed at low hydrothermal temperatures, and rutile formed at higher hydrothermal temperatures. The DSSC fabricated on the TiO_2 main-layer + TNTc scattering layer shows the highest conversion efficiency of 4.4% (0.63 Voc, 10.71 mA/cm^2 of Jsc, and 65.23% of fill factor) because of the increased Jsc due to the light-scattering effect. Compared to the scattering efficiency of rutile and anatase particles, the rutile particle-based scattering layer exhibited a slightly higher photocurrent density than the anatase-based one, which is associated with the higher refractive index of the rutile phase. In addition, the grain size of the rutile phase is larger than that of the anatase phase. The light-scattering abilities of these scattering layers also depend on the relative sizes of the particles in the layers. Eventually, the light-scattering effect of the large-sized TNTs enhanced the photocurrent density and overall conversion efficiency.

Acknowledgment

This study was supported by the Human Resources Development of the Korea Institute of Energy Technology Evaluation and Planning (KETEP) grant funded by the Korea government Ministry of Knowledge Economy (No. 20104010100510)

References

[1] Grätzel, M. (2004). *J. Photochem. Phorobiol, A. 164*, 3.
[2] O'Regan, B., & Grätzel, M. (2004). *Nature*, *353*, 737–740
[3] Hamann, T. W., Jensen, R. A., Martinson, A. B. F., Ryswyk, H. V., & Hupp, J. T. (2008). *Energy Environ. Sci. 1*, 66–78.
[4] Kong, F. T., Dai, S. Y., & Wang, K. J. (2007). *Adv. Opto Elect.* 75384.
[5] Xia, J., Masaki, N., Jiang, K., Wada, Y., & Yanagida, S. (2006). *Chem. Lett. 35*, 252.
[6] Ito, S., Liska, P., Comte, P., Charvet, R., Péchy, P., Bach, U., Schmidt-Mende, L., Zakeeruddin, S. M., Kay, A., Nazeeruddin, M. K., & Grätzel, M. (2005). *Chem. Commun*, 4351–4353.
[7] Peng, B., Jungmann, G., Jäger, C., Haarer, D., Schmidt, H. W., & Thelakkat, M., (2001), *Coord. Chem. Rev*, *248*, 1479–1489.
[8] Ito, S., Kitamura, T., Wada, Y., & Yanagida, S. (2003). *Sol. Energy Mater. Sol. Cells*, *76*, 3.
[9] Huang, S. Y., Schlichthörl, G., Nozik, A. J., Grätzel, M., & Frank, A. J. (1997). *J. Phys. Chem. B*, *101*, 2576–2582.
[10] Nissfolk, J., Fredin, K., Hagfeldt, A., & Boschloo, G. J. (2006). *Phys. Chem. B*, *110*, 17715–17718.
[11] Ito, S., Murakami, T. N., Comte, P., Liska, P., Grätzel, C., Nazeeruddin, M. K., & Grätzel, M. (2008). *Thin Solid Films.*, *516*, 4613–4619.
[12] Vargas, W. E. (2000). *J. Appl. Phys.*, *88*, 4079.
[13] Adachi, M., Murata, Y., Takao, J., Jiu, J., Sakamoto, M., & Wang, F. (2004). *J. Am. Chem. Soc.*, *126*, 14943–14949.
[14] Kang, S. H., Kim, J. Y., Kim, Y., Kim, H. S., & Sung, Y. E. (2007). *J. Phys. Chem., C 111*, 9614.
[15] Ito, S., Chen, P., Comte, P., Nazeeruddin, M. K., Liska, P., Pechy, P., & Grätzel, M. (2007). *Res. Appl.*, 10.1002, 768.
[16] Barbé, C. J., Arendse, C. J., Comte, P., Jirousek, M., Lenzmann, F., Shklover, V., & Grätzel, M. (1997). *J. Am. Ceram. Soc.*, *80*, 3157–3171.
[17] Park, N. G., van de Lagemaat, J., & Frank, A. J. (2000). *J. Phys. Chem. B.*, *104*, 8989–8994.